energies

MDPI

Article

Assessing the Influence of Fracture Networks on Gas-Based Enhanced Oil Recovery Methods

Riyaz Kharrat *, **Nouri Alalim** and **Holger Ott**

Department Petroleum Engineering, Montanuniversität Leoben, 8700 Leoben, Austria;
nouri.alalim@gmail.com (N.A.); holger.ott@unileoben.ac.at (H.O.)
* Correspondence: riyaz.kharrat@unileoben.ac.at

Abstract: Numerous reservoirs that play a significant role in worldwide petroleum production and reserves contain fractures. Typically, the fractures must form a connected network for a reservoir to be classified as naturally fractured. Characterizing the reservoir with a focus on its fracture network is crucial for modeling and predicting production performance. To simplify the solution, dual-continuum modeling techniques are commonly employed. However, to use continuum-scale approaches, properties such as the average aperture, permeability, and matrix fracture interaction parameters must be assigned, making it necessary to improve the fracture depiction and modeling methods. This study investigated a fractured reservoir with a low matrix permeability and a well-connected fracture network. The focus was on the impact of the hierarchical fracture network on the production performance of gas-based enhanced oil recovery methods. The discrete fracture network (DFN) model was utilized to create comprehensive two-dimensional models for three processes: gas injection (GI), water alternating gas (WAG), and foam-assisted water alternating gas (FAWAG). Moreover, dimensionless numbers were employed to establish connections between properties across the entire fracture hierarchy, spanning from minor to major fractures and encompassing the fracture intensity. The results indicate that the FAWAG process was more sensitive to fracture types and networks than the WAG and GI processes. Hence, the sensitivity of the individual EOR method to the fracture network requires a respective depth of description of the fracture network. However, other factors, such as reservoir fluid properties and fracture properties, might influence the recovery when the minor fracture networks are excluded. This study determined that among the enhanced oil recovery (EOR) techniques examined, the significance of the hierarchical depth of fracture networks diminished as the ratio of major (primary fracture) aperture to the aperture of medium and minor fractures increased. Additionally, the impact of the assisted-gravity drainage method was greater with increased reservoir height; however, as the intensity ratio increased, the relative importance of the medium and minor fracture networks decreased.

Keywords: fractures networks; foam-assisted water alternating gas; water alternating gas; gas injection; discrete fracture model introduction

Citation: Kharrat, R.; Alalim, N.; Ott, H. Assessing the Influence of Fracture Networks on Gas-Based Enhanced Oil Recovery Methods. *Energies* **2023**, *16*, 6364. https://doi.org/10.3390/en16176364

Academic Editors: Rasoul Mokhtari and Karen L. Feilberg

Received: 31 July 2023
Revised: 18 August 2023
Accepted: 31 August 2023
Published: 2 September 2023

1. Introduction

Natural fractured reservoirs (NFRs) are among the most common hydrocarbon reservoirs globally, containing more than 50% of the known oil and gas reserves [1]. NFRs are distinguished by an interconnected fracture network of high permeability and low storage capacity that serves as the primary flow path. In contrast, the rock matrix serves as the hydrocarbon source [2]. These reservoirs are well known for having poorer recoveries than their counterpart clastic reservoirs due to their production characteristics and geological heterogeneities [3–8]. Furthermore, the channeling and fingering of the injected fluid may be due to the complexity of the natural fracture networks [9]. Increasingly, NFR recoveries ensure a steady supply of resources to international oil markets. Consequently, redevelopment of currently producing fractured reservoirs requires maintaining the supply but with adequate fracture characterization and modeling [10]. Therefore proper fracture identification and characterization are essential for understanding fluid displacements, especially for improved and enhanced oil recovery [11,12]. Recent studies have focused on modeling and simulating fluid flow in fractured subsurface systems due to the potential hydrocarbon reserves in fractured reservoirs [13–17].

Among the enhanced oil recovery (EOR) methods, gas injection (GI) has a wide range of applications in NFRs for various reasons, especially the availability and good injectivity of gas compared with water-based EOR methods. Based on the reservoir conditions, the immiscible or miscible gas injection might result in a successful EOR process [18]. However, gas injection might benefit these types of reservoirs if operated in the gas-assisted gravity drainage (GAGD) mode [6,10]. According to Silva and Maini, 2016 [19], the storage and transmissibility capacities, as well as the direction and intensity of the fracture, are the key features of the GAGD process. Since the reservoir's production potential is determined by the storage and transmissibility capacity, the fracture intensity and direction describe the flow pattern in the reservoir. Hence, information and implementation of fracture intensity and direction are important in assessing the GAGD recovery mode. The fracture intensity is thereby a controlling parameter for EOR and gas storage in a fractured reservoir, i.e., for carbon dioxide sequestration. A high fracture density forms massive continuous flow paths and makes the specific geometry of the fracture insignificant [5].

The gravity override and unfavorable mobility are the main causes of the poor sweep efficiency during gas injection. Consequently, it is necessary to utilize certain chemicals, like surfactants, or techniques, such as gas-based EOR processes, which involve alternating water and gas injection in cycles. Foam can potentially serve as an alternative method for decreasing gas mobility and redirecting gas flow away from fractures and toward the reservoir matrix. Nevertheless, the precise mechanisms of foam injection and its interaction with different fracture types remain inadequately explored, especially in fractured carbonate reservoirs characterized by high salinity, divalent ions, and elevated temperatures [9,18]. Therefore, gas-based methods, such as WAG and FAWAG methods, were introduced to overcome the deficiencies of gas injection [15,20–22]. However, the modeling and simulation of WAG and FAWAG include additional complexities, such as three-phase flow, especially for carbonate reservoirs. It has its challenges due to the flow functions that define the physics of fluid displacement in the fracture and the matrix, particularly the three-phase transfer function [16].

In the simulation of fractured reservoirs, simplifying the model by excluding, including, or homogenizing fractures is a common practice. However, the heterogeneous distribution of fracture characteristics can have a considerable impact on the fluid flow behavior, leading to variations in recovery performance [16]. Additionally, the behavior of produced fluids over the injection period can also be affected [23], making fracture characteristics essential in the history-matching process of such reservoirs. Notably, a case study of a giant carbonated reservoir with a production history spanning over ninety years demonstrated improved prediction accuracy when all fracture networks were included, except for hairline fractures, which had a minor effect [12]. Similarly, Aljuboori et al. (2020) [6] confirmed the significance of fracture characteristics in history matching for a carbonate reservoir with a 40-year production history, emphasizing the importance of accurate fracture identification and modeling.

Water flooding processes were also shown to be influenced by the types of fractures, with a remarkable observation that a relatively small number of fractures accounted for a major portion of the injected water flow [14]. In a recent study involving a 2D model with major, medium, and minor fracture networks, it was observed that oil was displaced primarily in the fractures during the early production period, while drainage from the matrix occurred later. During this initial production period, the fracture network's impact on recovery was more pronounced, while the minor fractures had a comparatively smaller effect [12].

Therefore, precise evaluation of both the matrix and fractures is crucial for a comprehensive approach, and accurate identification and modeling of fractures may significantly enhance the history-matching process and overall understanding of gas-based enhanced oil recovery methods in fractured reservoirs. Limited studies were reported on the impact of the fracturing effect on the gas-based EOR processes; hence, more work is needed. Generally, the dual continuum approach is used for modeling and simulation, where fracture properties are subjected to upscaling and homogenization [24–27]. In certain cases, it may be necessary to reassess the fracture characteristic inputs based on the recovery process that has been implemented. The possibility of modeling different discrete fracture networks was recently introduced without further upscaling processes [28]. This approach can thoroughly facilitate the study of different fracture types and their impact on production. This work aimed to investigate the impact of fracture network sets on the recovery of gas-based processes using the recent CMG DFN modeling approach.

2. Methodology

A two-dimensional vertical slice model was constructed to study the impact of the fracture type on recovery for gas-based EOR methods. Vertical and horizontal injection schemes were used to investigate whether fracture networks were sensitive to each propagation direction. Moreover, an extended vertical model with two slices was used to investigate the assisted drainage mode. The model dimensions, grid size, and related properties are shown in Table 1. A single porosity domain was used to represent the reservoir rock with an isotropic matrix permeability of 1 mD with a matrix porosity of 20%. Three sets of fracture networks were defined in each model: major, medium, and minor sets of fractures with maximum and minimum apertures of 2 and 0.20 mm, respectively. In Figure 1, the exact locations of the fractures and the wells can be observed. A heterogeneous distribution was assumed for the fracture aperture, i.e., fracture permeability.

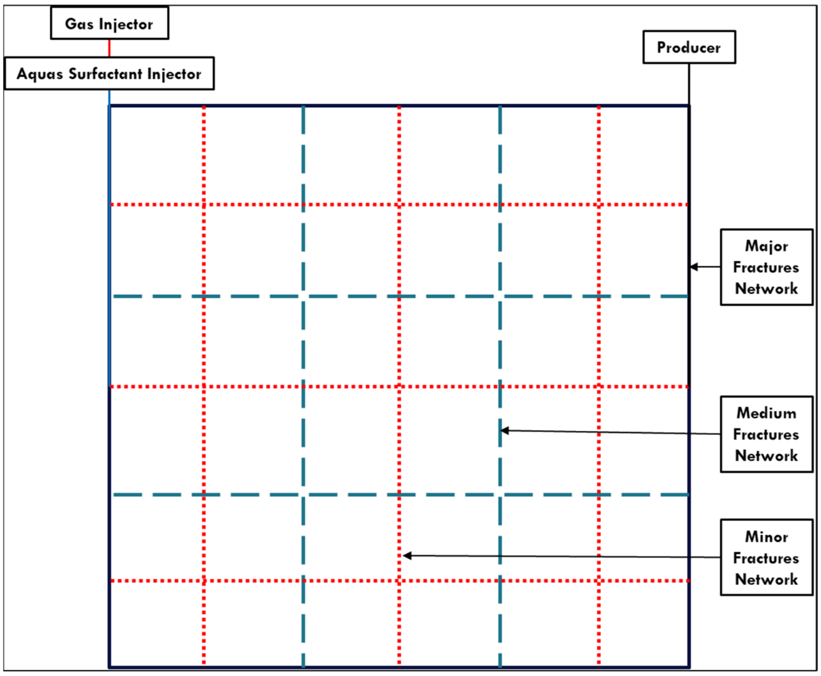

Figure 1. Model configuration with three fracture types.

Table 1. Models configurations and description.

Model Name	Dimensions			Grids Number in Each Direction			Porosity	Permeability		
	Meter						%	mD		
	X	Y	Z	X	Y	Z	-	X	Y	Z
2D vertical slice	15	1	15	67	1	67	0.2	1	1	1
Extended 2D vertical slice	15	1	30	67	1	134	0.2	1	1	1

With the CMG 2020.1 update, it is possible to model various discrete fracture networks without requiring additional upscaling procedures. The discrete fracture segment (DFS) and discrete fracture unit (DFU) were introduced for the DFN. The control volume segments are embedded by defining the explicit location of the DFN. Each fracture plane intersects directly with the corresponding matrix grid to form a connected network. The DFN is discretized based on the shape, orientation, aperture, and permeability of a DFU. Then, based on the intersection with the matrix grid, each DFU is discretized into a DFS. The flow ability of the fracture is then determined based on the fracture aperture and permeability [24]. In this approach, the flow description within fractures does not require data on capillary pressure and relative permeability but is connected to the matrix. Thus, this study utilized this approach to examine the effect of different fracture network sets on the production and recovery processes.

Dimensionless numbers, namely, R_{m12} (major-to-medium aperture ratio), R_{m13} (major-to-minor aperture ratio), and R_n (number of major fractures-to-total number of major and medium fractures) were introduced to characterize the system heterogeneity based on the fracture apertures, as defined in Equations (1)–(3), respectively [13]. Additionally, these dimensionless numbers allowed us to descriptively describe the fracture properties and their influence on the recovery factor for each recovery process.

$$R_{m12} = \frac{Major\ fracture\ apeature}{Medium\ fracture\ apeature} \tag{1}$$

$$R_{m13} = \frac{Major\ fracture\ apeature}{Minor\ fracture\ apeature} \tag{2}$$

$$R_n = \frac{Number\ of\ Major\ fractures}{Total\ number\ of\ Major\ and\ Medium\ fractures} \tag{3}$$

For each case, the fracture permeability was varied by varying the fracture aperture using the cubic law. Three categories were defined to cover a wider range of properties for each set of fracture networks, from coarse to fine. The properties for the different categories and the resulting dimensionless number are summarized in Table 2. As can be seen, the major fractures' aperture and permeability were constant in all categories. The fracture permeability was selected to be higher than the matrix for all the cases to avoid any numerical issues, as recommended by Wong et al. [29] with a similar embedded district fracture model (EDFM).

Different combinations of fracture types were implemented in the constructed 2D model. The fracture set effect was in terms of major only, major–medium, and major–medium–minor with 1, 9, and 36 blocks, respectively. For the CGI, horizontal and vertical displacement modes were considered, while only horizontal displacement was used for the FAWAG and WAG. In the WAG and FAWAG processes, the water was injected at a half height of the matrix block to avoid gravity segregation and promote the interaction between the phases. Thus, water flowed in the lower part and the gas in the upper part model. The workflow of the study is illustrated in Figure 2. Based on these models, several cases with different objectives were defined to investigate the properties change for these non-major fracture networks and compare it to the case when these networks were excluded. In all the cases, two pore volumes were injected.

Table 2. Properties of the three categories.

Properties	Fractures Aperture mm			Dimensionless Numbers		Fractures Permeability Darcy		
Category	Major	Medium	Minor	R_{m12}	R_{m13}	Major	Medium	Minor
1	2.00	1.60	0.80	1.25	2.50	4.00	2.56	0.64
2	2.00	0.80	0.40	2.50	5.00	4.00	0.64	0.16
3	2.00	0.40	0.20	5.00	10.00	4.00	0.16	0.04

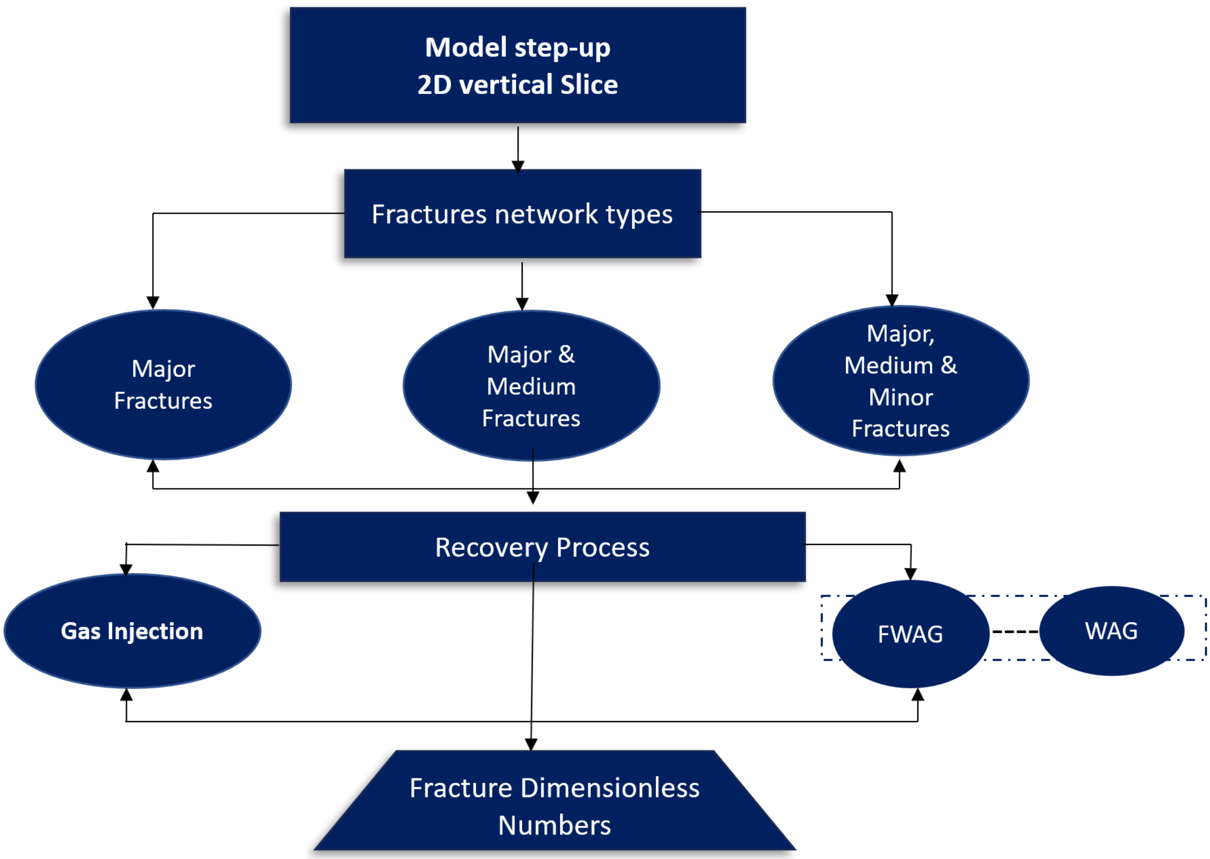

Figure 2. Workflow of the study for the effect of the fracture's networks.

At first, the immiscible gas injection was investigated using the IMEX-CMG black oil model. Then, the FAWAG and WAG processes with a ratio of one to two cycles were studied using the GEM-CMG compositional model. For foam, the GMSMO85 CMG model was adjusted to simplify the modeling process and maintain this study's main target of investigating the fracture networks' effect on the recovery process. The fluid parameters, relative permeability, and capillary curves were chosen and aligned with those observed in a field in the Middle East fractured reservoir. The fluid properties of the gas injection process and foam are summarized in Table 3.

Table 3. Oil fluid properties used for gas injection and foam.

Gas Injection Fluid Model			Foam Model CMG	
Parameter	**Value**	**Unit**	**Component**	**Mole**
GOR	155	m^3/m^3	C1	0.50
Pb	362.6	psi	C3	0.03
Bg	0.0043	m^3/sm^3	C6	0.07
Bo	1.42	m^3/sm^3	C10	0.20
µg	0.042	cp	C15	0.15
µo	0.76	cp	C20	0.05

In this research, we employed the implicit-texture local-equilibrium approach to investigate the foam injection process, following the methodology established by Ma et al. [30]. The foam quality, representing the ratio of the gas rate to the total fluid rate, was defined based on the work of Luo and Mohanty [7]. For this study, we utilized the foam empirical parameters and relevant equations previously documented by Alalim [23].

This approach involved the generation of foam in the presence of a surfactant component in an aqueous and a gas phase. It assumed the presence of foam wherever surfactant was present. The foam properties were characterized by several empirically determined parameters, like the foam mobility reduction factor [28].

3. Results and Discussion

The impacts of the fracture types on the GI, WAG, and FAWAG processes were analyzed and discussed using the dimensionless numbers defined earlier. Various simulation scenarios were explored, with some cases involving only a primary (major) fracture network as the basis of the simulation, while others included an additional major fracture. Additionally, certain simulations incorporate connected medium and minor fracture networks. Moreover, both horizontal and vertical displacement modes were taken into account.

3.1. Gas Injection

3.1.1. Horizontal Displacement Mode

At first, vertical wells in a single block (one slice) were used to investigate the gas injection mechanism, where the displacement was from left to right. The gas injection results for the three categories are discussed in this section. Figure 3 shows the resulting oil saturation profile at 0.5, 1, 1.5, and 2 pore volumes (PVs) for the three fracture network categories defined above; only major fracture, major and medium fracture, and all fractures were included. Based on the observed results, the gas flowed first in the primary fractures network, surrounded the matrix block, and gradually drained the matrix. The gas flow was parallel to the flow direction in the horizontal fractures by including the medium and minor fractures. In contrast, the gas flow in the vertical fractures was subjected to re-infiltration of the oil from one matrix block to another and the gravity effect. The oil gradually drained as the gas saturation increased and surrounded the matrix block. By including all fracture networks, slight differences can be observed, even in the first category, explaining the small effect of the minor fracture network. This is in agreement with the observed results published for a single porosity model and matrix block, especially for the second- and third-category networks, where smaller blocks were used, and the aperture size of the non-major fractures was small [6,16].

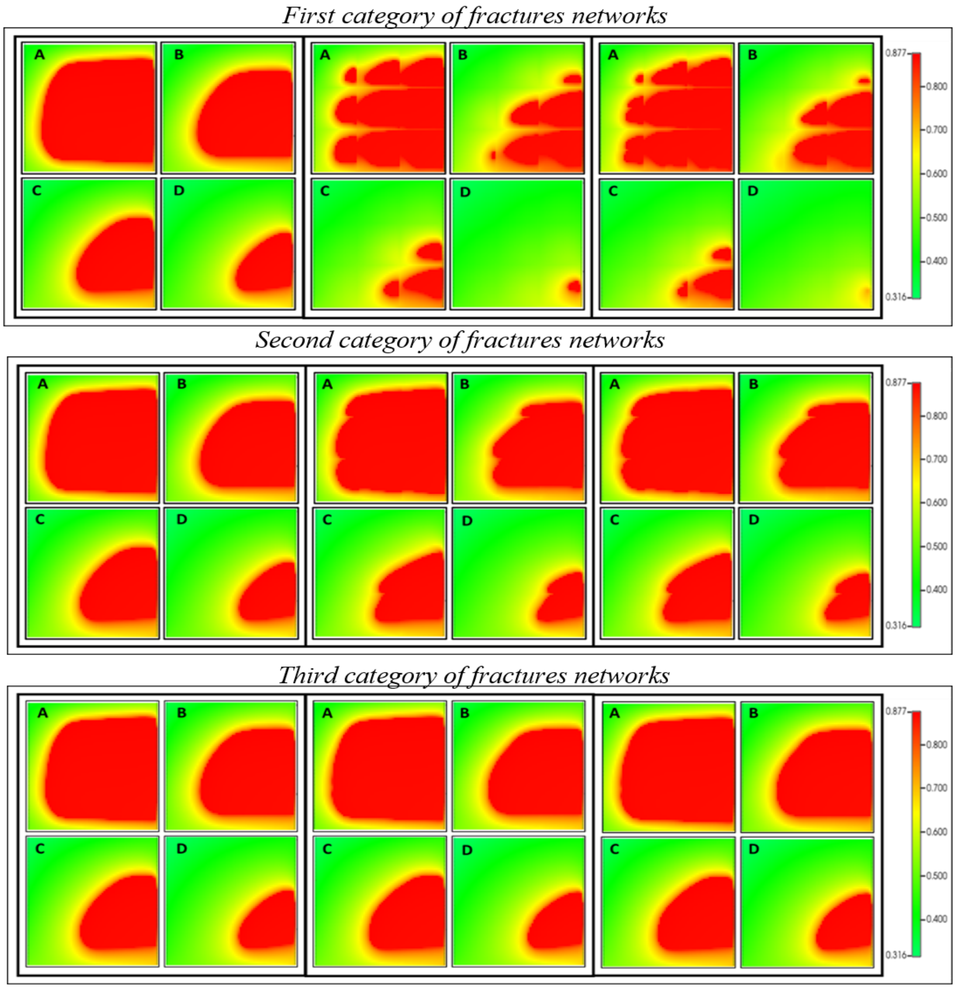

Figure 3. Oil saturation profile for gas injection process (**left**) only major fracture network; (**middle**) major and medium fracture networks; (**right**) major, medium, and minor fracture networks, at A: 0.5 PV, B: 1 PV, C: 1.5 PV, and D: 2 PV (oil in red and gas in green).

The comparison for the recovery factor of the first category indicates that the difference after the complete injection of 1 PV could reach 11% in the first category and resulted in an underestimation of the recovery factor when the medium and minor fracture network was excluded (Figure 4). In the second category, the difference magnitude decreased to reach 3%. In the third category, almost no difference was found. This indicated that their impact on recovery decreased as the aperture size of the non-major fracture networks decreased.

Figure 5 displays the gas–oil ratio of the gas injection process for the first category. The simulated GOR indicates an entirely different behavior with the inclusion of the medium and minor fracture networks. When considering only the major fractures network, the produced gas volume was overestimated during the initial injection phase, from gas breakthrough to 1.6 pore volumes, but was underestimated in later stages. When the medium and minor fractures were included, the impact was more noticeable during the first pore volume injection and at the end of the process impact; hence, all fractures should be considered. In the second category, excluding the non-major fracture network, the results of the GOR were overestimated; however, the magnitude and behavior differed from the first. On the other hand, the inclusion of minor fractures did not change the picture. This indicates a threshold exists from which fractures may be ignored and do not alter the displacement behavior.

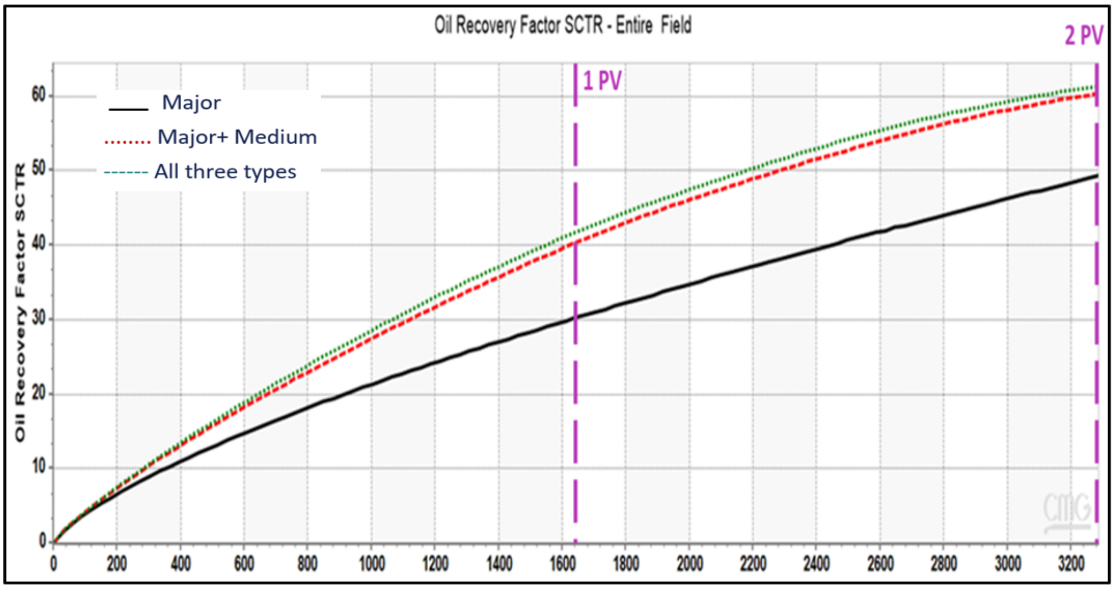

Figure 4. Oil recovery factor for gas injection process (horizontal mode—first category).

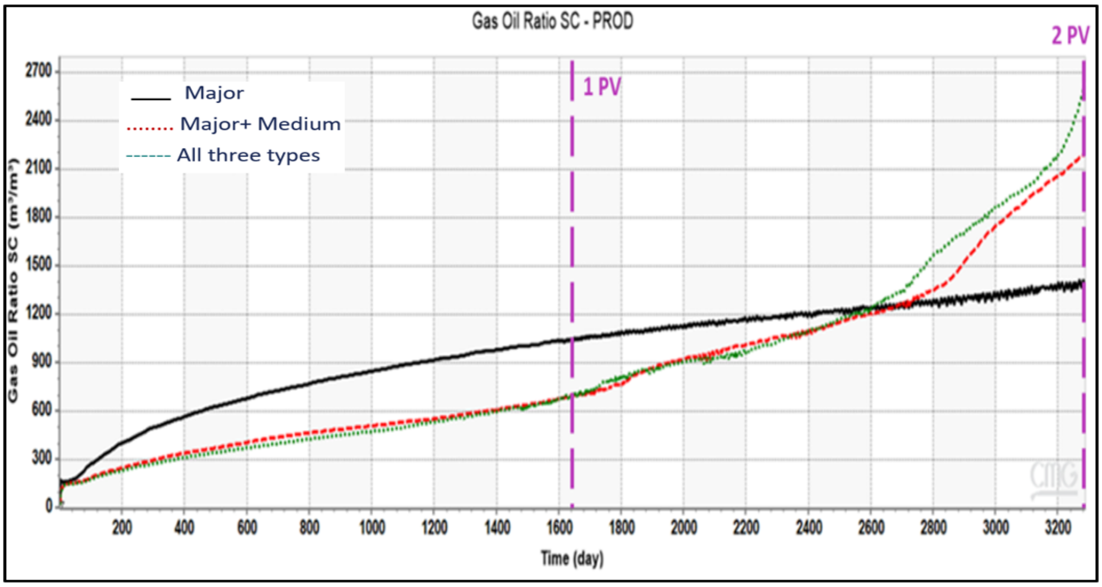

Figure 5. GOR for gas injection process (horizontal mode—first category).

Narrow fractures, which may have comparable capillary pressures to the matrix because of liquid bridging, can lead to significant production volume discrepancies during gas injection processes if not considered, as noted by Harimi et al. [31]. The significance of incorporating various sets of fracture networks was established for all three categories, highlighting the need to consider these fracture networks carefully.

3.1.2. Assisted Gravity Drainage Model

This section assumed a horizontal well configuration to study gas-assisted gravity drainage effects. The injection well was positioned at the top of the block, while the production well was at the bottom. The saturation profile of the first category is shown in Figure 6. The gas moved in the major fractures network and surroundings of the matrix block, where it was gradually draining the matrix. Incorporating medium fractures allowed for the observation of gas flow in the vertical fractures, as they were oriented parallel to the flow direction. The gas flow in the horizontal fractures resulted in the initiation of multiple mechanisms, such as capillary continuity, oil re-infiltration, and gravity drainage. However, as the gas saturation increased in the fractures, the matrix block was slowly drained.

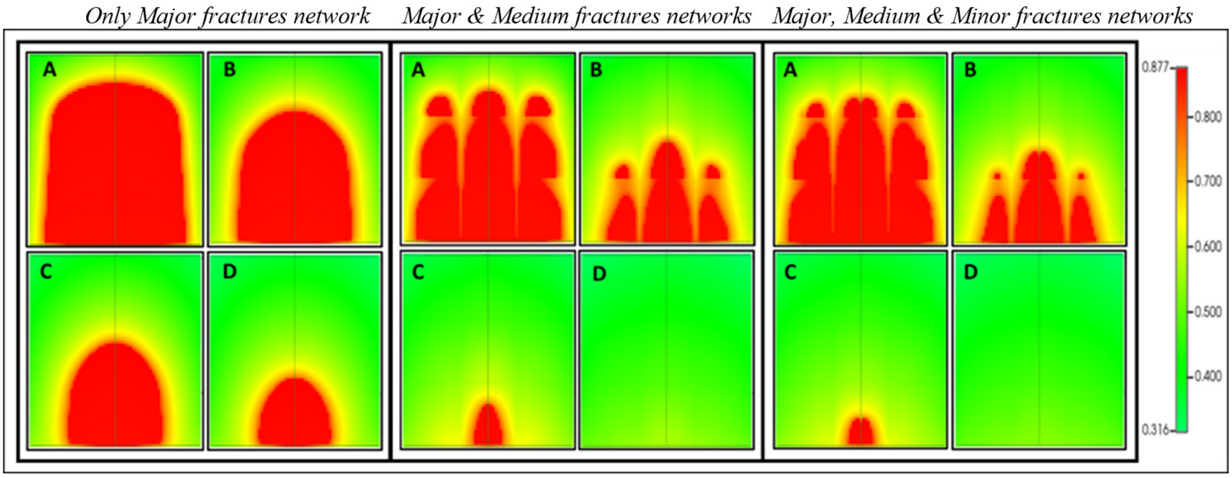

Figure 6. First category oil saturation profile of gas injection process (gravity drainage mode) (**left**) only major fractures network; (**middle**) major and medium fractures networks; (**right**) major, medium, and minor fractures networks at A: 0.5 PV, B: 1 PV, C: 1.5 PV, and D: 2 PV (oil in red and gas in green).

3.1.3. Extended 2D Vertical Slice

Two vertical slices were used to investigate the impact of the reservoir height and fractures network on the gas-assisted gravity drainage. This was also done to confirm the standard model's observations and capability to capture the production behavior. Comparable recovery performance was observed for the major and non-major fractures, similar to the standard model (one-slice model); however, the effects of capillary continuity and gas breakthrough across different fractures were better observed from the saturation profile. The capillary continuity phenomenon, as experimentally verified by Harimi et al. in 2019, is demonstrated in Figure 7, where a liquid bridge is observed to form between two sections of the horizontal fractures. The formation of this bridge between the blocks was the cause of the phenomenon. The high oil saturation at the lower section of the upper block crossed the fracture into the upper part of the lower block. When the non-major fractures were not included, the capillary continuity was maintained for a longer time, even after the injection of one pore volume. However, the capillary continuity was interrupted faster when the medium and minor fractures were included.

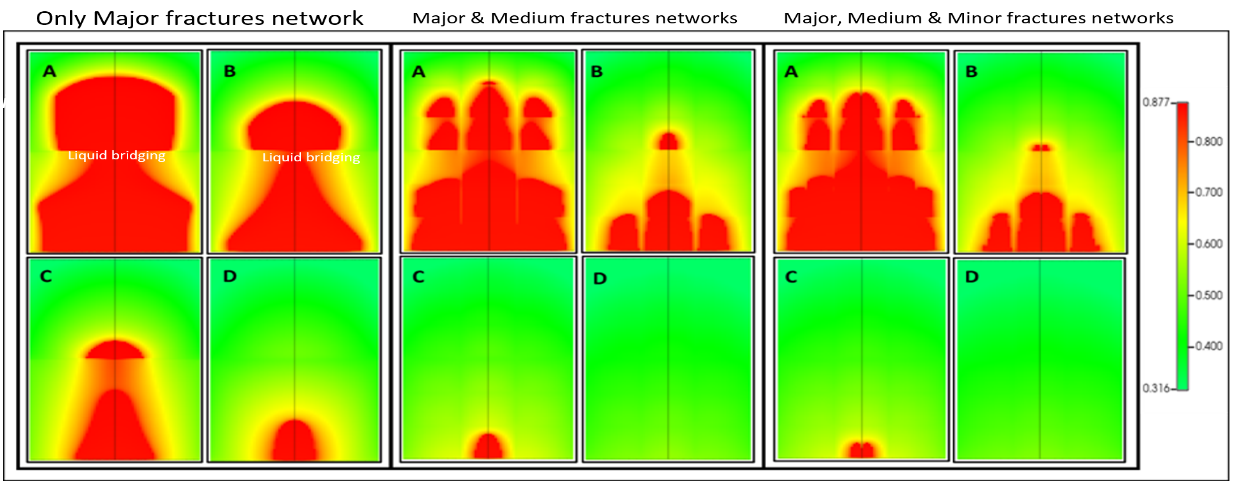

Figure 7. First category oil saturation profile of gas injection process (extended gravity drainage mode) of the first category at A: 0.5 PV, B: 1 PV, C: 1.5 PV, and D: 2 PV (oil in red and gas in green).

3.2. Foam-Assisted WAG

The simulation of the FAWAG process was conducted for the three categories based on horizontal displacement, and the differences between the oil recovery, GOR, water cut, and gas and water saturation were analyzed and compared. The results of the first category are discussed in greater detail because of its greater sensitivity.

The major difference in the oil recovery was observed between 0.37 pore volumes and 1.58 pore volumes in the first category of fracture networks (Figure 8). No difference was observed in the first cycle of the aqueous phase (capillary-driven imbibition) and the third gas phase (gravity-driven) cycle when the non-major fractures were included or excluded. It should be noted that in the third aqueous phase, the oil saturation almost reached the residual oil saturation. Hence, the contribution of the medium fracture network to the recovery was around 5 to 10%. It should be noted that by introducing the non-major fracture networks, the size of the matrix block became smaller, which might result in different gravitational and capillary forces interactions since the interaction of these forces depends on the matrix blocks' size and shape [16].

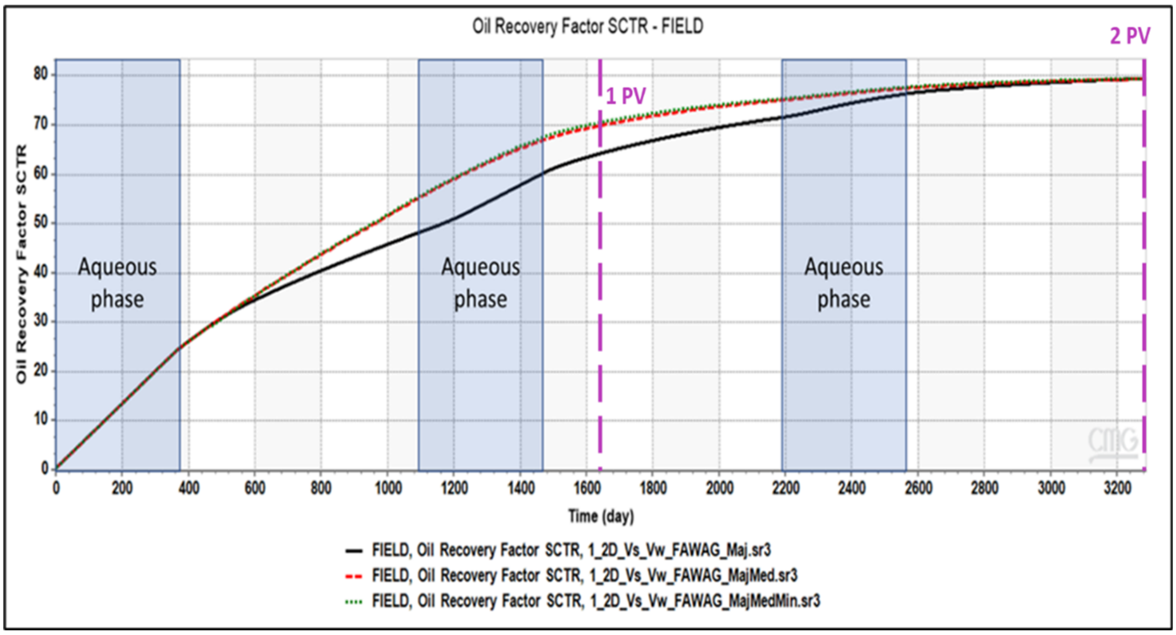

Figure 8. Oil recovery vs. time of the FAWAG process in the first category.

As shown in Figure 9, the GOR profile over the two cycles shows that excluding the non-major fractures marked a slight overestimation of the produced gas in the first cycle. However, the difference was more noticeable upon the second cycle's commencement, especially in the last gas injection cycle. At the end of the injection period, the major fracture case shows a lower GOR. In comparison, the recovery factor at the end of the second cycle was consistent across all cases. GOR analysis provides a better understanding of fluid behavior and the influence of different fracture types, even in the case of minor fractures with small apertures. Theoretical and experimental evidence shows a diversion mechanism in which the foam flows in non-major fractures rather than major fractures within a fractured medium [32,33].

The impact was more pronounced for the water cut, as shown in Figure 10. Although the first cycle showed little variation in all scenarios, the second cycle, which involved the aqueous phase, led to a noticeable increase in water production in the major fracture network case. However, the opposite trend was observed during the remaining process, where all fractures were included. These observations indicate the fracture network's importance in displacing the injected and produced fluids in the early and late stages of production.

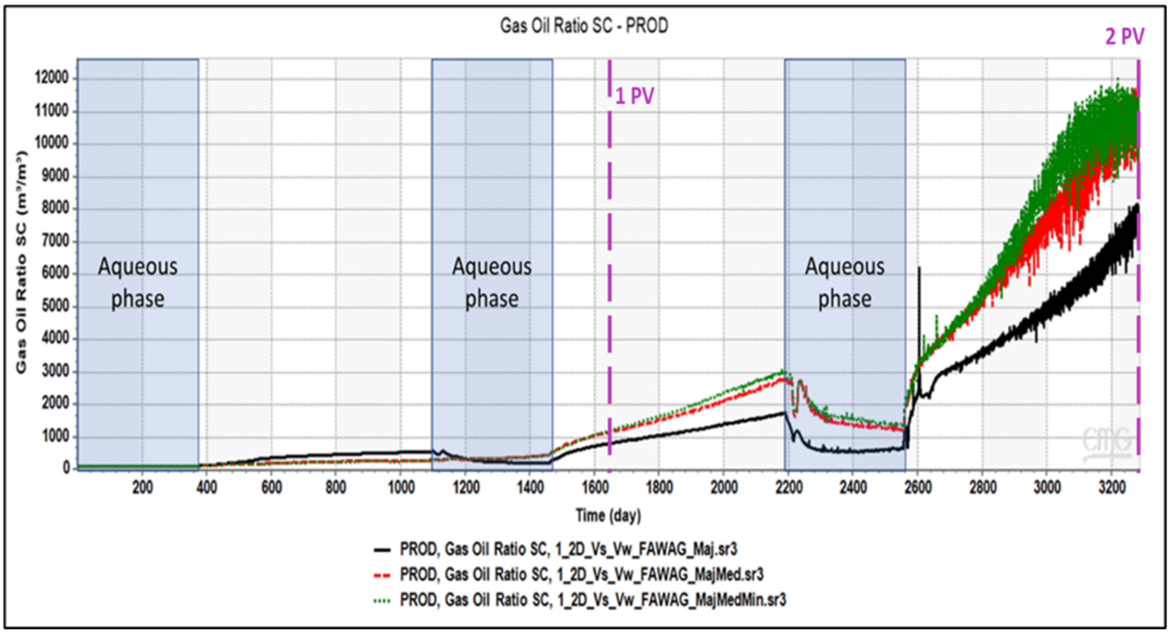

Figure 9. GOR vs. time of the FAWAG process in the first category.

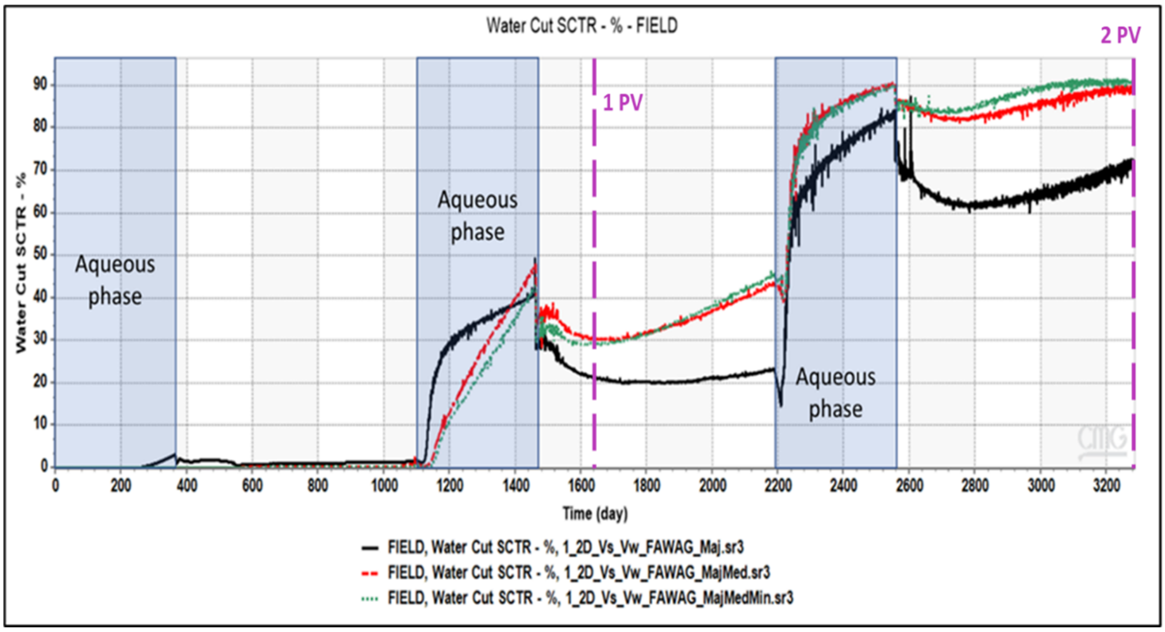

Figure 10. Water cut vs. time of the FAWAG process of the first category.

The influence of minor and medium fractures on the simulation of the gas injection process was more evident when incorporated or excluded, as is evident from the gas–oil ratio and water cut profiles. Therefore, the gas and water saturation profiles might better describe the observed influence of the fracture types on production.

The gas and water saturation demonstrated notable profile differences attributed to governing recovery mechanisms. The gas saturation profile for the FAWAG in the first category for the three cases is shown in Figure 11. The green and red denote oil and gas, respectively. As seen in the case of the major facture only, the gas phase diffused from the fracture into the matrix, resulting in the oil flow from the matrix block(s). More gas was in contact with oil when the medium and minor fractures were included in the model, resulting in higher recovery. In the water cycle, the imbibition and re-imbibition were more pronounced when the non-major fractures were included (Figure 12).

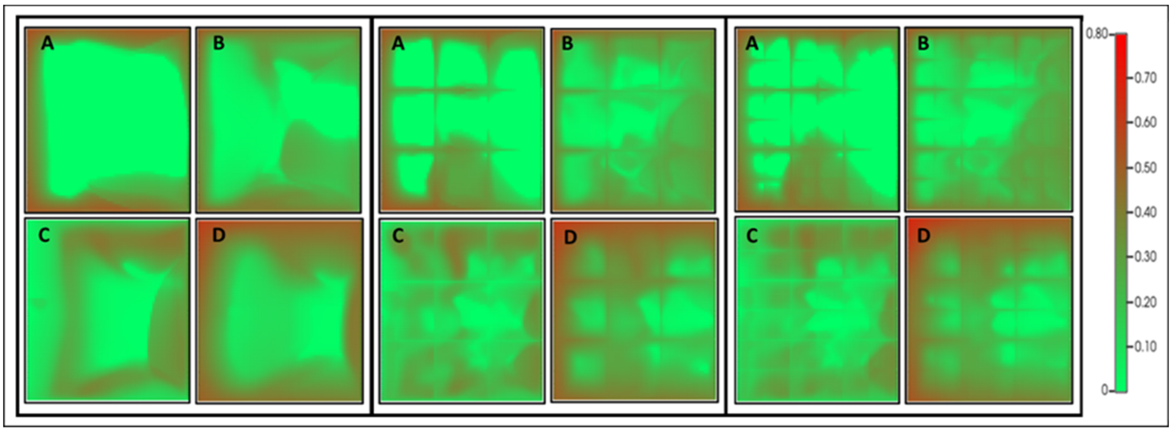

Figure 11. Profile of the gas saturation of FAWAG process in the first category (**left**) only major fractures network; (**middle**) major and medium fractures networks; (**right**) major, medium, and minor fractures networks at A: 0.5 PV, B: 1 PV, C: 1.5 PV, and D: 2 PV (gas in red and oil in green).

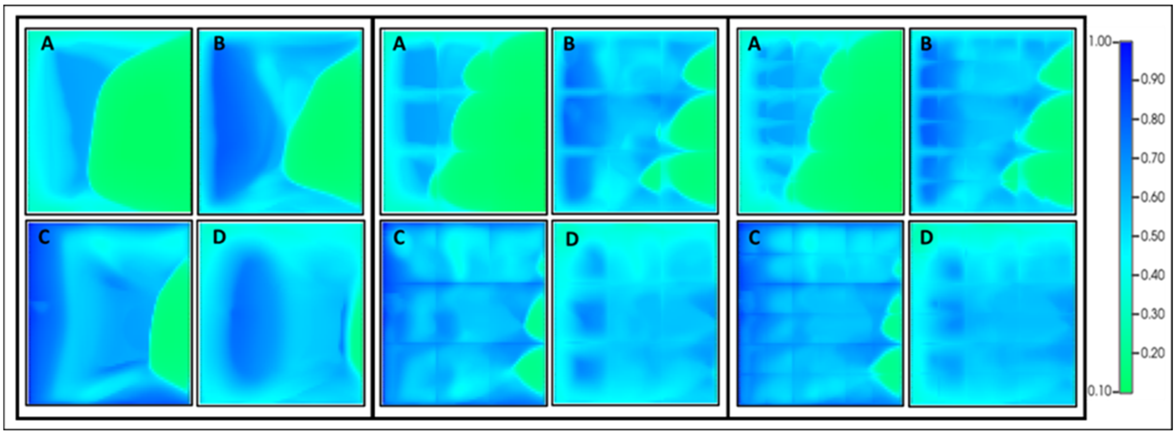

Figure 12. Profile of water saturation of FAWAG process in the first category (**left**) only major fractures network; (**middle**) major and medium fractures networks; (**right**) major, medium, and minor fractures networks at A: 0.5 PV, B: 1 PV, C: 1.5 PV, and D: 2 PV (water in blue and oil in green).

Permeability and dry-out interpolator parameters models were used to examine the degree of foam generation [28]. Based on the relative permeability indicator, the foam (blue) was generated first in the major fractures and then in non-major fractures (Figure 13). It is important to note that blue signifies foam production, while red does not. The gas phase's relative permeability was modified when the necessary condition for foam generation started forming. The same observation was found when the dry-out interpolator parameter model was used (Figure 14). In the figure, areas highlighted in red indicate where drying-out occurred, while green indicates where the formation did not experience any drying-out conditions. The blue regions in the figure correspond to locations where foam had not yet formed.

The second and third categories show similar observations regarding oil recovery, GOR, and water cuts. However, the difference compared with the first category was less pronounced, as exemplified by the oil recovery of the second category (Figure 15).

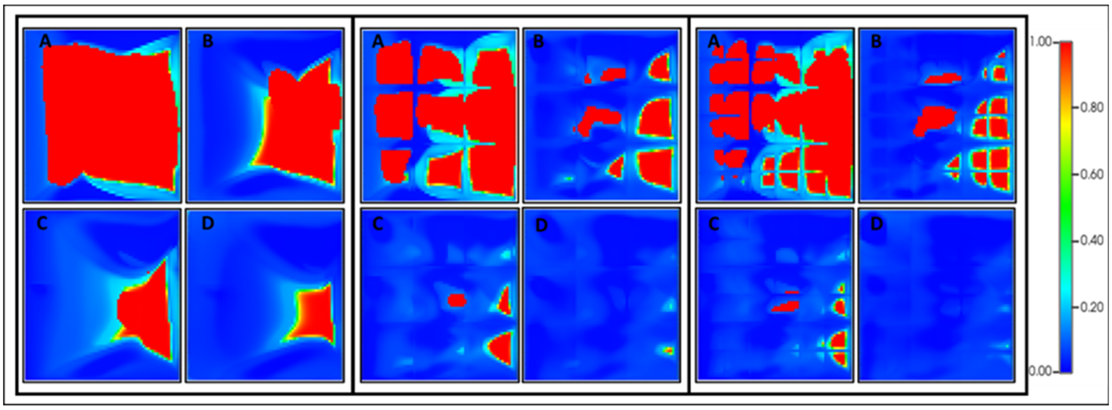

Figure 13. Profile of the relative permeability interpolator (in blue) of FAWAG process in the first category (**left**) only major fractures network; (**middle**) major and medium fractures networks; (**right**) major, medium, and minor fractures networks at A: 0.5 PV, B: 1 PV, C: 1.5 PV, and D: 2 PV.

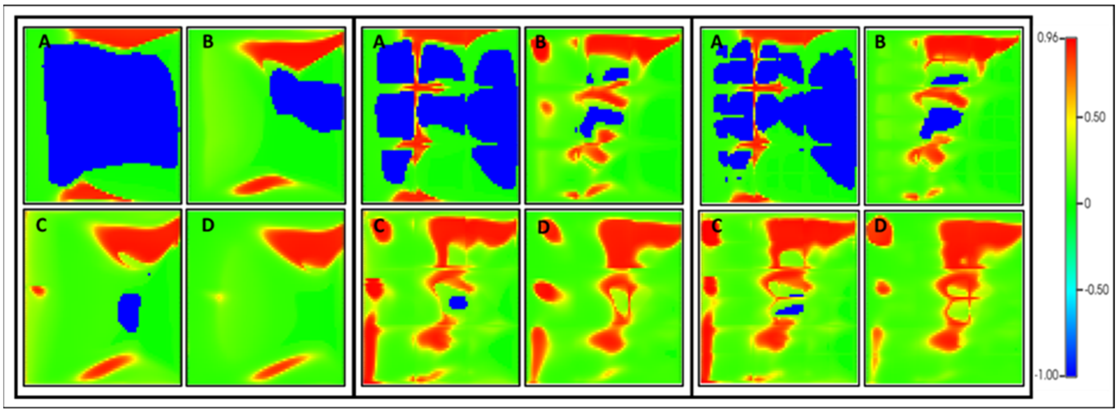

Figure 14. Profile of the dry-out interpolation parameter (in red) of FAWAG process in the first category (**left**) only major fractures network; (**middle**) major and medium fractures networks; (**right**) major, medium, and minor fractures networks at A: 0.5 PV, B: 1 PV, C: 1.5 PV, and D: 2 PV.

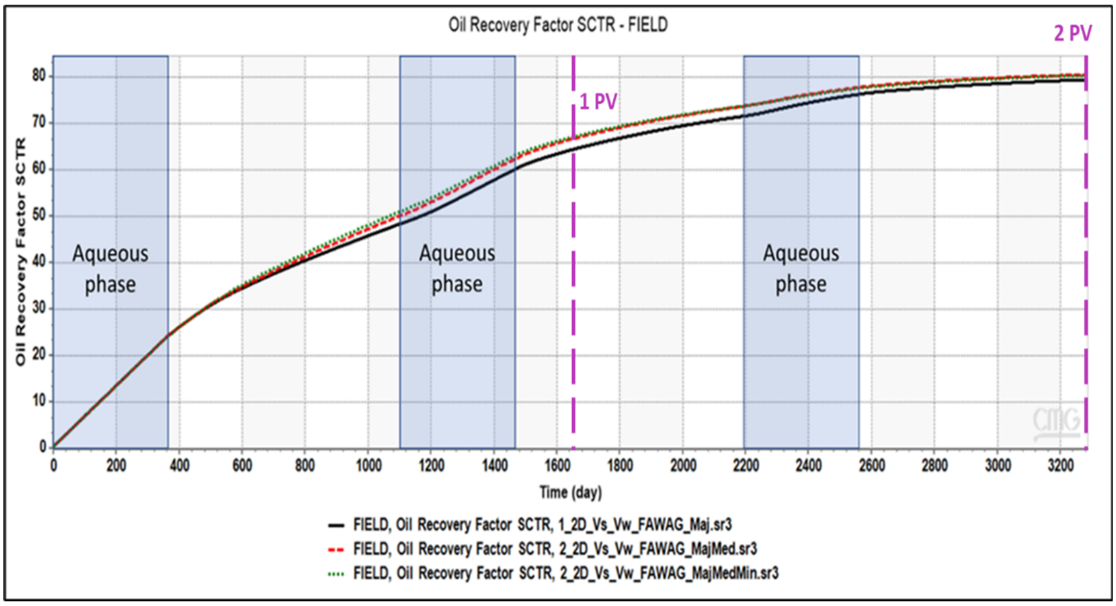

Figure 15. Oil recovery vs. time of the FAWAG process (second category of fractures networks).

The GOR behavior difference was noticeable in the last cycle when the medium and the minor fractures networks were included. In contrast, no difference was observed in the previous cycles, as shown in Figure 16.

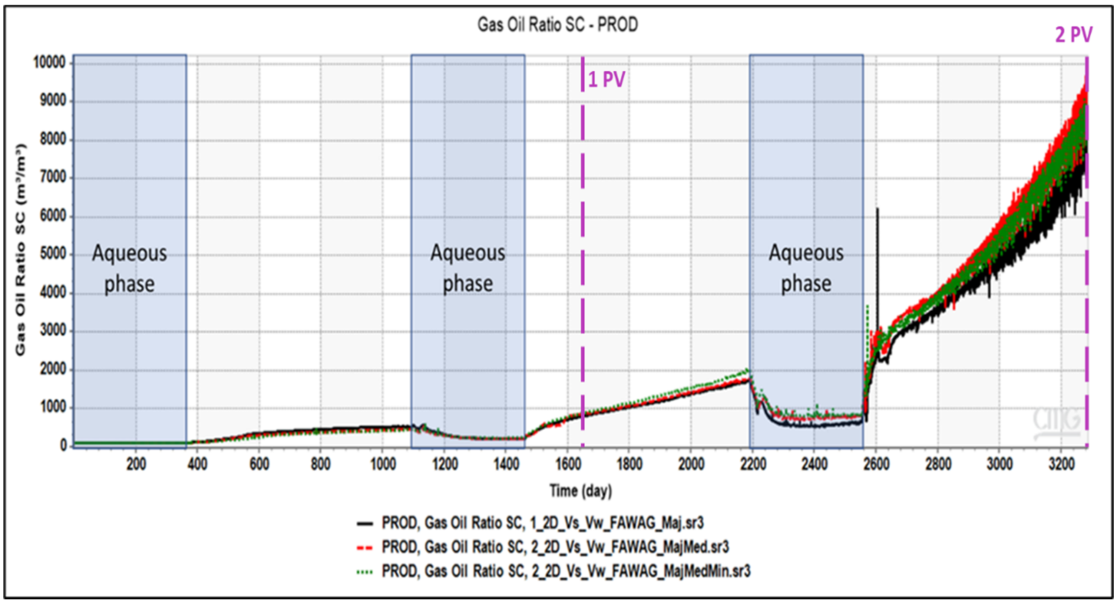

Figure 16. GOR vs. time of the FAWAG process (second category of fractures networks).

The GOR and water cut profile differences in the second category of fracture networks were more noticeable in the last cycle compared with the previous cycles when the medium and minor fracture networks were included (Figure 16). However, the difference in the water cut was slightly more pronounced than the GOR profile, as shown in Figure 17.

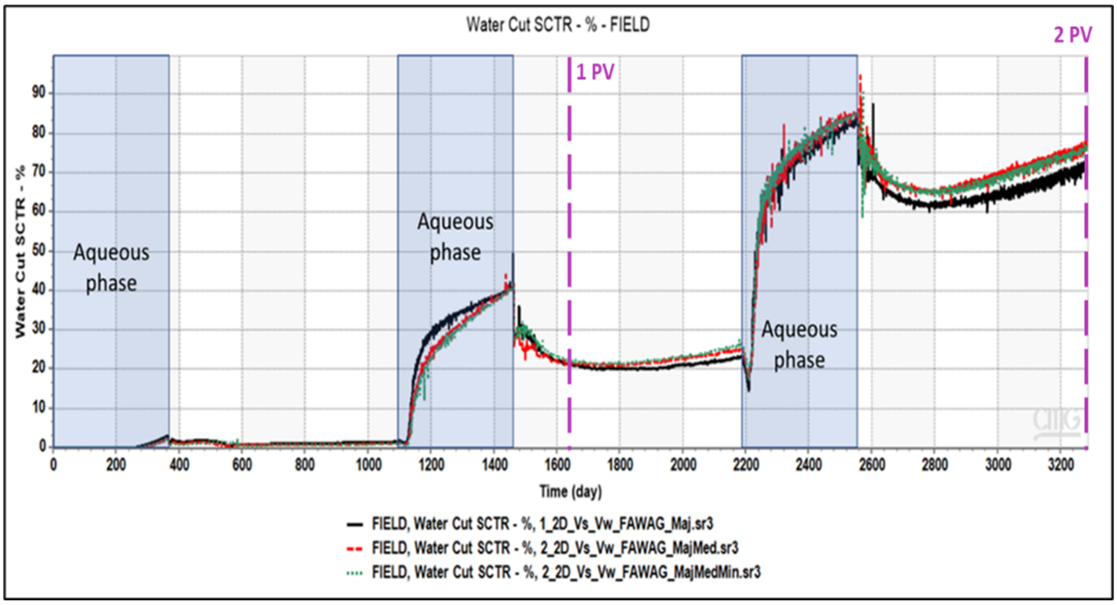

Figure 17. Water cut vs. time of the FAWAG process (second category of fractures networks).

For the third category, the magnitude of the recovery and the behavior trend were almost the same for the major and non-major fracture cases. Consequently, the medium and minor fracture networks exerted a lesser influence on the displacement of the injected and produced fluids. This was based on the comparable behavior and magnitude observed for

GOR and water cut for these cases. Moreover, the gas and water saturation profiles indicate that the gas flow performance within the fracture networks remained largely unaffected by the non-major fracture networks. As evidenced by the findings from the studied cases, the significance of non-major fracture networks in influencing recovery and fluid behavior during gas injection diminished from the second to the third category.

3.3. WAG Process

The impact of the fracture types on the WAG process was simulated with the same cycle ratio used for the FAWAG process. The results of both methods for the major and non-major cases of the first category are given in Figure 18. An underestimation of the foam generation's positive impact in improving recovery was observed for the major fracture case. The influence could only be observed at the injection of more than one pore volume. The impact of the foam becomes evident when the medium and minor fractures are added to the major fractures, resulting in the inclusion of all fractures. However, minor fractures had minimal impact, and the medium fractures network largely drove the additional recovery contribution.

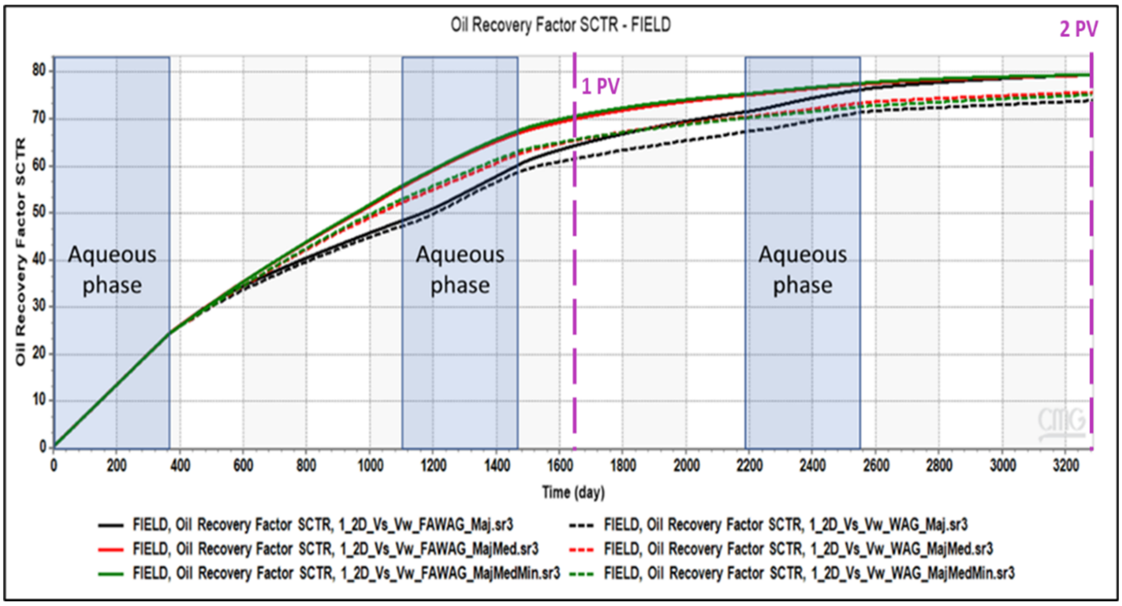

Figure 18. FAWAG and WAG oil recovery factor in the first category of fracture networks.

As expected, lower oil recovery resulted in the WAG process than the FAWAG process for the three fractured studied cases. However, the positive impact of the foam was perceived almost only after the second cycle of the aqueous phase injection when the non-major fracture was not included. This observation emphasized the importance of including fracture networks, especially the medium ones, in the recovery process. Hence, the impact of fracture type might be process dependent.

The study findings suggest that the efficacy of the EOR techniques examined was subject to the type and characteristics of the fracture network. Specifically, major fractures exert a greater influence compared with minor ones. The recovery factor for the horizontal displacement mode at one pore volume in the defined dimensionless numbers context is depicted in Figure 19. The impact of minor fractures on the recovery was only seen at low R_{m12} and R_{m13}, as presented by the first category set. Similar results were found for the gravity drainage mode. As indicated by the thirst category set, the minor fractures' effect was nil when these two dimensionless numbers increased. The same trend was observed for the FAWAG process, as seen in Figure 20. However, the impact of the medium fracture on the recovery was more pronounced in the gas injection process than in the FAWAG process. Around 10% of the gas injection was attributed to the gas injection compared with the 5% for the FAWAG.

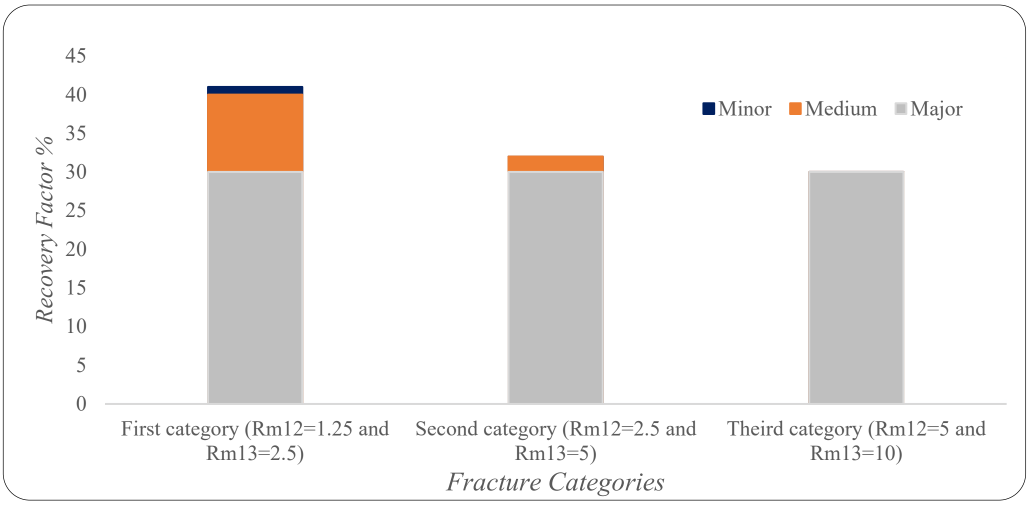

Figure 19. Gas injection recovery contribution of the three categories at one pore volume (horizontal displacement: Rn = 0.5).

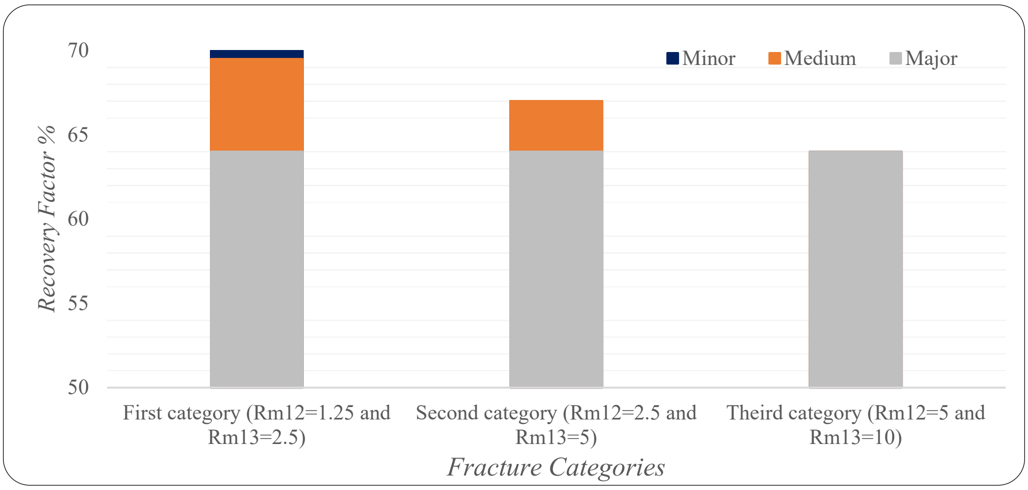

Figure 20. FAWAG recovery contribution of the three categories at one pore volume (Rn = 0.5).

The results of the extended vertical model for the first category in which the fracture intensity (R_n) was increased are given in Figure 21. When there was an increase in the intensity of major to medium fractures, the significance of other fracture networks decreased. More contribution was attributed to the non-major fractures. A 10% additional recovery resulted from the medium fractures than the one-slice vertical injection mode. This was related to block height increase and was attributed to the gravity drainage enhancement.

The fracture networks' contribution to the recovery factor for WAG, FAWAG, and GI processes is shown in Figure 22, where the same oil model was used. The minor fracture type had the minimum recovery contribution to the GI and WAG processes. The recovery was mostly affected by the major and, to a lesser extent, medium fracture. The equilibrium between capillary/gravity forces in the matrix blocks and gravity/viscous forces in fracture controlled the recovery performance in fractured reservoirs [10,20]. The FAWAG process was reported to be matrix–fracture interaction dependent and more sensitive to permeability contrast, fracture density, and matrix block heights than WAG injection [10]. Furthermore, when evaluating gas-based EOR techniques for gas-invaded regions in fractured reservoirs, Gugl et al. [15] found that fracture permeability had the greatest impact on oil recovery. Specifically, lower fracture permeability facilitated gas penetration into the matrix blocks. The impact of fracture types can be considered process dependent, possibly due to the different dominant forces for each process. The difference also highlights the fluid properties' influence on the fracture network's impact on the EOR process, which needs further investigation.

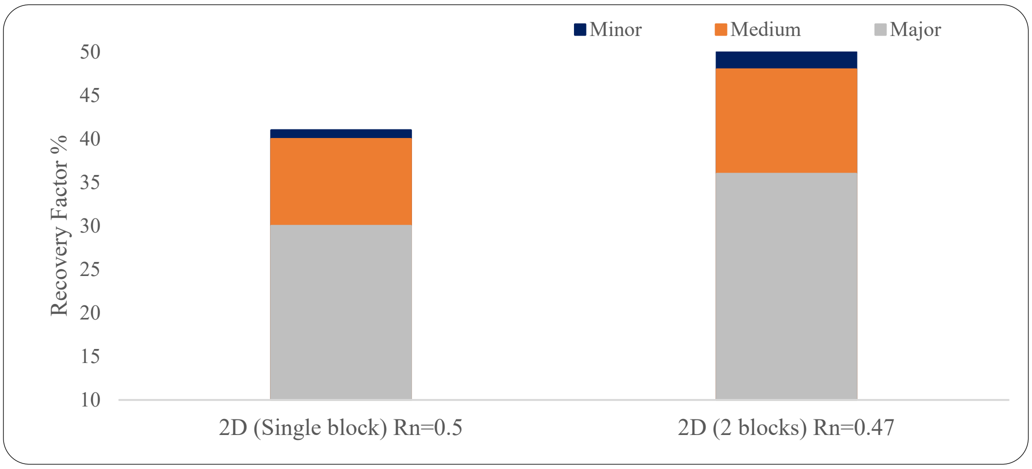

Figure 21. Gas injection recovery contribution of the fracture types of the vertical and extended 2D models.

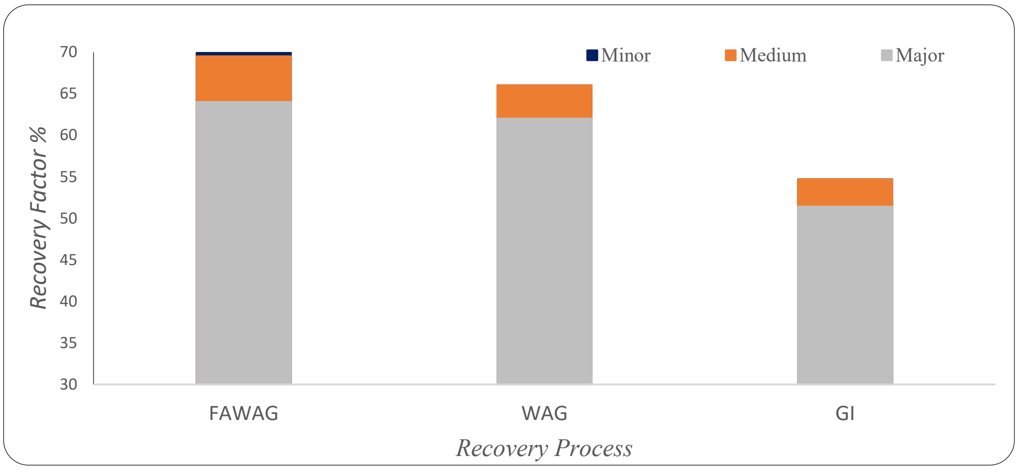

Figure 22. Fractures networks' effect on WAG, FAWAG, and GI recovery (Rn = 0.50).

4. Summary and Conclusions

In recent decades, fractured reservoirs have been a significant challenge in oil and gas reservoir modeling because the properties of fractures and matrix blocks substantially impact the flow performance. The continuous geoscience development in reservoir characterization, especially in fracture network recognition and interpretation, can significantly improve reservoir description and provide a more realistic reservoir model [34]. In addition, the fracture types' contribution to production and the related mechanisms in the primary or later stages of production can be well understood if the interaction between the fracture network and matrix blocks is precisely modeled. Any simplification or homogenization with the assumption of a single set of fracture networks can undermine the production mechanisms, as is usually done in the conventional dual-porosity or dual-permeability models [23,35,36]. The observed results emphasized the impact of fracture networks on the gas-based EOR processes. The impact magnitude for excluding the different types of fracture networks depends on multiple effects that include the recovery process and the reservoir fluids' fluid properties. Also, the literature has established that fracture characteristics and heterogeneity of local apertures do impact foam generation and flow distribution [37,38]. Consequently, more consideration is needed for the FAWAG process modeling in fractured reservoirs. In addition, dimensionless numbers used in this work might be further integrated with force-based numbers to evaluate the production mechanisms in fractured reservoirs.

This study investigated the impact of fracture types on the performance of gas-based EOR methods. Major, medium, and minor fracture types were employed for studying the different combination effects of the gas injection, WAG, and FWAG processes. The medium fractures contributed more to production for the FAWAG process than the WAG and GI based on the studied models, whereas the minor fractures had a minimum effect. According to the analyzed enhanced oil recovery techniques results, the significance of non-major fracture networks diminished as the major-to-medium and major-to-minor aperture ratios increased. Hence, increasing the aperture ratios decreased the relative importance of medium and minor fractures. However, the degree of impact increased with the height block. Moreover, the increase in the major to medium fracture intensity decreased the non-major impact on the studied processes. The major fractures had the highest impact on the recovery magnitude, while the minor ones had a minor contribution. However, the difference in the gas–oil ratio and water cut was more noticeable than in the oil recovery when the non-major fractures were included.

Author Contributions: Conceptualization, R.K.; formal analysis, N.A.; investigation, N.A.; methodology, R.K. and N.A.; software, N.A.; supervision, R.K. and H.O.; writing—review and editing, R.K. and H.O. All authors have read and agreed to the published version of the manuscript.

Funding: This research received no external funding.

Data Availability Statement: Not applicable.

Acknowledgments: The authors would like to acknowledge the support provided by the Computer Modeling Group (CMG).

Conflicts of Interest: The authors declare no conflict of interest.

References

1. Saidi, A.M. *Reservoir Engineering of Fractured Reservoirs: Fundamental and Practical Aspects*; Total: Paris, France, 1987.
2. Van Golf-Racht, T. Developments in Petroleum Science. In *Fundamentals of Fractured Reservoir Engineering*; Elsevier Scientific Publishing Company: Amsterdam, The Netherlands, 1982.
3. Allan, J.; Sun, S.Q. Controls on Recovery Factor in Fractured Reservoirs: Lessons Learned from 100 Fractured Fields. In Proceedings of the SPE Annual Technical Conference and Exhibition, Denver, CO, USA, 5–8 October 2003; Volume 18.
4. Kharrat, R.; Mahdavi, S.; Ghorbani, D. A Comprehensive EOR Study of a Highly Fractured matured field-Case Study. In Proceedings of the 74th EAGE Conference and Exhibition incorporating EUROPEC 2012, Copenhagen, Denmark, 4–7 June 2012; Volume 153311.
5. Agada, S.; Geiger, S.; Doster, F. Wettability, hysteresis, and fracture–matrix interaction during CO_2 EOR and storage in fractured carbonate reservoirs. *Int. J. Greenh. Gas Control* **2016**, *46*, 57–75. [CrossRef]
6. Aljuboori, F.A.; Lee, J.H.; Elraies, K.A.; Stephen, K.D. Effect of fracture characteristics on history matching in the Qamchuqa reservoir: A case study from Iraq. *Carbonates Evaporites* **2020**, *35*, 87. [CrossRef]
7. Luo, H.; Mohanty, K.K. Modeling Near-Miscible Gas Foam Injection in Fractured Tight Rocks and Its Challenges. *Energies* **2021**, *14*, 1998. [CrossRef]
8. Kharrat, R.; Ott, H. A Comprehensive Review of Fracture Characterization and Its Impact on Oil Production in Naturally Fractured Reservoirs. *Energies* **2023**, *16*, 3437. [CrossRef]
9. Xu, Z.-X.; Li, S.-Y.; Li, B.-F.; Chen, D.-Q.; Liu, Z.-Y.; Li, Z.-M. A review of development methods and EOR technologies for carbonate reservoirs. *Pet. Sci.* **2020**, *17*, 990–1013. [CrossRef]
10. Kharrat, R.; Zallaghi, M.; Ott, H. Performance quantification of Enhanced Oil Recovery Methods in fractured reservoirs. *Energies* **2021**, *14*, 4739. [CrossRef]
11. Guerriero, V.; Mazzoli, S.; Iannace, A.; Vitale, S.; Carravetta, A.; Strauss, C. A permeability model for naturally fractured carbonate reservoirs. *Mar. Pet. Geol.* **2013**, *40*, 115–134. [CrossRef]
12. Pejic, M.; Kharrat, R.; Kadkhodaaie, A.; Azizmohammadi, S.; Ott, H. Impact of fracture types on the oil recovery in naturally fractured reservoirs. *Energies* **2022**, *5*, 7321. [CrossRef]
13. Gong, J.; Rossen, W.R. Modeling flow in naturally fractured reservoirs: Effect of fracture aperture distribution on dominant sub-network for flow. *Pet. Sci.* **2017**, *14*, 138–154. [CrossRef]

14. Gong, J.; Rossen, W.R. Characteristic fracture spacing in primary and secondary recovery for naturally fractured reservoirs. *Fuel* **2018**, *223*, 470–485. [CrossRef]
15. Gugl, R.; Kharrat, R.; Shariat, A.; Ott, H. Evaluation of Gas-based EOR Methods in Gas Invaded Zones of Fractured Carbonate Reservoir. *Energies* **2022**, *15*, 4921. [CrossRef]
16. Elfeel, M.A.; Al-Dhahli Geiger, S.; van Dijke, M.I.J. Fracture-matrix interactions during immiscible three-phase flow. *J. Pet. Sci. Eng.* **2016**, *143*, 171–186. [CrossRef]
17. Al Karfy, L.; Kharrat, R.; Ott, H. Mechanistic study of the carbonated smart water in carbonate reservoirs. *Greenh. Gases Sci. Technol.* **2021**, *11*, 661–681. [CrossRef]
18. Mogensen, K.; Masalmeh, S. A review of EOR techniques for carbonate reservoirs in challenging geological settings. *J. Pet. Sci. Eng.* **2020**, *195*, 107889. [CrossRef]
19. Silva, R.R.; Maini, B. Evaluation of Gas-Assisted Gravity Drainage GAGD in Naturally Fractured Reservoirs NFR. In Proceedings of the SPE Improved Oil Recovery Conference, Tulsa, OK, USA, 11–13 April 2016.
20. Heeremans, J.; Esmaiel, T.; Kruijsdijk, C.V. Feasibility Study of WAG Injection in Naturally Fractured Reservoirs. In Proceedings of the SPE/DOE Symposium on Improved Oil Recovery, Tulsa, OK, USA, 22–26 April 2006; Volume 100034, p. 10.
21. Gbadamosi, A.O.; Kiwalabye, J.; Juni, R.; Augustine, A. A review of gas enhanced oil recovery schemes used in the North Sea. *J. Pet. Explor. Prod. Technol.* **2018**, *8*, 1373–1387. [CrossRef]
22. Ayoub, M.; Saaid, I.B.; Shabib-asl, A. Comprehensive Review of Foam Application during Foam Assisted Water Alternating Gas (FAWAG) Method. *Res. J. Appl. Sci. Eng. Technol.* **2014**, *8*, 1896–1904.
23. Alalim, N. Impact of Fractures Networks on Gas-Based EOR Methods. Ph.D. Thesis, University of Leoben, Leoben, Austria, 1 July 2022.
24. Bourbiaux, B. Fractured Reservoir Simulation: A Challenging and Rewarding Issue. *Oil Gas Sci. Technol.-Rev. De L'Institut Français Du Pétrole* **2010**, *65*, 227–238. [CrossRef]
25. Kasiri, N. Status of Dual-Continuum Models for Naturally Fractured Reservoir Simulation. *Pet. Sci. Technol.* **2011**, *29*, 1236–1248. [CrossRef]
26. Lei, Q.; Latham, J.-P.; Tsang, C.-F. The use of discrete fracture networks for modeling coupled geomechanical and hydrological behavior of fractured rocks. *Comput. Geotech.* **2017**, *85*, 151–176. [CrossRef]
27. Bosma, S.; Hajibeygi, H.; Tene, M.; Tchelepi, H.A. Multiscale finite volume method for discrete fracture modeling on unstructured grids (MS-DFM). *J. Comput. Phys.* **2017**, *351*, 145–164. [CrossRef]
28. CMG. *GEM 2020.11 User Guide*; Computer Modelling Group Ltd.: Calgary, AB, Canada, 2020.
29. Wong DL, Y.; Doster, F.; Geiger, S.; Francot, E.; Gouth, F. Fluid Flow Characterization Framework for Naturally Fractured Reservoirs Using Small-Scale Fully Explicit Models. *Transp. Porous Media* **2020**, *134*, 399–434. [CrossRef]
30. Ma, K.; Ren, G.; Mateen, K.; Morel, D.; Cordelier, P. Modeling Techniques for Foam Flow in Porous Media. *SPE J.* **2015**, *20*, 453–470. [CrossRef]
31. Harimi, B.; Masihi, M.; Ghazanfari, M.H. Characterization of Liquid Bridge in Gas/Oil Gravity Drainage in Fractured Reservoirs. *Iran. J. Oil Gas Sci. Technol.* **2019**, *8*, 73–91.
32. Kovscek, A.R.; Tretheway, D.C.; Persoff, P.; Radke, C.J. Foam flow through a transparent rough-walled rock fracture. *J. Pet. Sci. Eng.* **1995**, *13*, 75–86. [CrossRef]
33. Haugen, A.; Fernø, M.A.; Graue, A. Experimental Study of Foam Flow in Fractured Oil-Wet Limestone for Enhanced Oil Recovery. *SPE Reserv. Eval. Eng.* **2012**, *15*, 218–228. [CrossRef]
34. Wenli, Y.; Sharifzadeh, M.; Yang, Z.; Xu, G.; Fang, Z. Assessment of fracture characteristics controlling fluid flow performance in discrete fracture networks (DFN). *J. Pet. Sci. Eng.* **2019**, *178*, 1104–1111. [CrossRef]
35. Xu, Y.; Sepehrnoori, K. Development of an Embedded Discrete Fracture Model for Field-Scale Reservoir Simulation With Complex Corner-Point Grids. *SPE J.* **2019**, *24*, 1552–1575. [CrossRef]
36. Yan, X.; Huang, Z.; Yao, J.; Li, Y.; Fan, D. An efficient embedded discrete fracture model based on mimetic finite difference method. *J. Pet. Sci. Eng.* **2016**, *145*, 11–21. [CrossRef]
37. Shojaei, J.M.; de Castro, A.R.; Meheust, Y.; Shokri, N. Dynamics of foam flow in a rock fracture: Effects of aperture variation on apparent shear viscosity and bubble morphology. *J. Colloid Interface Sci.* **2019**, *552*, 464–475. [CrossRef]
38. Osei-Bonsu, K.; Shokri, N.; Grassia, P. Fundamental investigation of foam flow in a liquid-filled Hele-Shaw cell. *J. Colloid Interface Sci.* **2016**, *462*, 288–296. [CrossRef]